

Using Artificial Neural Networks and the Monte Carlo Method for the Regulation of Flow Generators by the Rotation Variation

Afonso Henriques Moreira Santos, Paulo Marcelo Tasinaffo

Abstract— This paper presents a motor-pump assembly's energy balance in the presence of a frequency inverter to predict potable water power functioning at variable speed. In order to carry out the system's energy balance, we consider the operating characteristics of the pump unit, the physical and geometrical characteristics of the hydraulic network, and the monthly consumption of drinking water of the households or consumers benefiting from this network. The mathematical tools used in this simulation were the combinations of the Monte Carlo method and the neural networks. We used the neural networks to predict the motor-pump assembly's behavior through the interpolation of the Hill Diagram and for the recognition of the Moody diagram used in determining the system's loss of load. Finally, the flexibility of the neural networks reduces the necessary empirical data collection. Moreover, to perform the simulation in other hydraulic systems besides in this work, it is recommended to transpose the result.

Index Terms— Monte Carlo Method, Artificial Neural Networks, Fluid Mechanics, Hill Diagram, Moody Diagram, Energy Conservation, Flow Generators

I. INTRODUCTION

This article bestowed the energy balance of a motor-pump set in the presence of a frequency inverter to predict the power of the hydraulic pump operating at variable rotation. Furthermore, regarding the motor-pump set's operating characteristics, the physical and geometric characteristics of the hydraulic network, and the monthly consumption of drinking water in the homes benefited by this network, bring out the system's energy balance. The mathematical tools used in this simulation were the combinations of the Monte Carlo method with artificial neural networks. Next, predicting the motor-pump behavior by neural networks is set through the interpolation of the hill diagram and for the recognition of the Moody diagram used to determine the head loss of the system. The technical terminologies, the description of the operation of hydraulic installations, and the load loss calculation can be found in [1]-[3]. During the hydraulic systems simulation process, besides this study, and to reduce the necessary empirical data collection, the transposition of the results should consider the flexibility of the neural networks.

Figure 1 illustrates the basic operating principles of the simulator developed here. As can be seen, a graphic editor allows the isometric entry of the hydraulic network. A neural network with feedforward architecture (e.g., [4]-[7]) predicts

the behavior of the motor-pump set (15CV) through the interpolation of the hill diagram. Hydrometric measurements performed in the field allowed the computer to store the statistical behavior of drinking water consumers of the hydraulic installation studied here. In this way, the machine will be able to apply the Monte Carlo method (see [8], [9], [10], [11]) to perform the energy balance of the system with the pump working, both at variable rotation as for constant rotation. The method of transposition of results will allow predicting the behavior of water consumption of any other hydraulic installation without the need for new hydrometric measurements.

Thus, we divided this work as follows: after the start with off brief study case explanation section II will carry out a bibliographic review of the existing literature, then, section III will carry out the theoretical development of the Monte Carlo method used in this simulation. Next, section IV develops the methodology for translating the results to simulate new hydraulic installations without the need for new hydrometric measurements. Section V presents a brief theoretical summary of artificial neural networks and how they work. Section VI describes qualitatively, from a physical point of view, the most relevant characteristics of the hill diagram of centrifugal pumps in general.

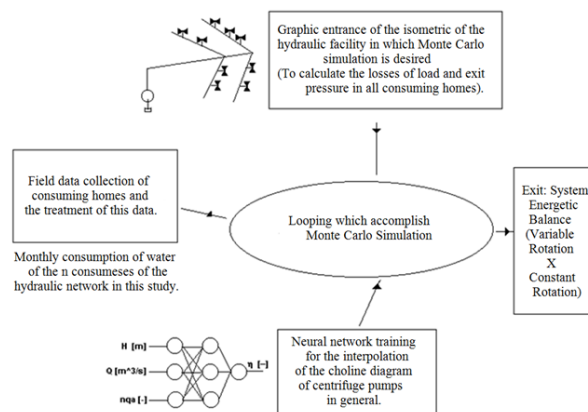


Fig. 1 Simplified scheme of the simulator developed in this work.

Section VII briefly describes the graphic and algebraic principles used to determine the head losses of consumers in the hydraulic network. Section VIII explains a complete computational algorithm how was mentioned in the previous sections, involving everything that has already discussed. Lastly, section IX presents a practical result of this simulation carried out in Bairro Vista Verde, located in the city of Itajubá/Brazil. Still, in section IX, a simulation with a constant rotation of the centrifugal pump is compared with a simulation with rotation variation. In the end, the conclusions

Paulo Marcelo Tasinaffo, Departamento de Ciência da Computação, Instituto Tecnológico de Aeronáutica (ITA), São José dos Campos/SP, Brazil.

Afonso Henriques Moreira Santos, Instituto de Recursos Naturais, Universidade Federal de Engenharia de Itajubá (UNIFEI), Itajubá/MG, Brazil.

and final comments on this work are in section X. It is important to note that we use MATLAB® to produce the simulation.

II. LITERATURE REVIEW

The design of industrial pipelines and the calculation of load loss can be found in [1]-[3]. An Introduction to the design of flow machines in [1] reproduces a concise theoretical text. However, this bibliographic review will focus more precisely on the subjects and works of the Monte Carlo method and artificial neural networks. With this purpose in mind, below, some articles and books describing the Monte Carlo methods will be described, followed by some articles and books on the artificial neural networks' theoretical development.

Several books and articles are describing the Monte Carlo method mathematically (e.g., [8]-[14]). However, minimal knowledge of statistics is necessary to understand this method better. A classic statistical book in the area is due to Papoulis (1965) in [12]. Simultaneously, [13] and [14] characterize two modern and recent applications using the Monte Carlo method combined with the theory of artificial neural networks. In [13], the Monte Carlo method is used to previously estimate the mean quadratic training error of a feedforward neural network designed with unbalanced training patterns. In [14], the Monte Carlo method is used together with an MLP neural network to calculate the area of forest reserves from drone photos.

The Monte Carlo method is a way of solving problems using random numbers. Computer simulation models widely use this method.

In this context, simulation is a technique that emulates the operation of a real-world system as that system evolves time-tested. An adequate way to simulate the behavior of the type of variables to be analyzed is to develop a simulation model using discrete-event probability distributions known as the Monte Carlo method.

As described in [8], forego the complex analytical mathematical models modeled the interactions between nuclear particles in favor of modeling only the rules and statistics that govern each stage of the process. Starting from a uniform statistical distribution and then mapping it to distributions of interest to the given problem, it was possible to process multiple decision chains (simulations) and then extract relevant results with precision compatible with analytical methods.

On the other hand, Artificial intelligence has allowed significant advances in the area of computing. One of the most successful approaches is artificial neural networks, which would enable, for example, the recognition of writing, image processing, modeling of nonlinear dynamic systems, applications in control theory, etc. An excellent introduction to the theory of artificial neural networks can be found in [4], [15], [16]. An essential starting point in the study of artificial neural networks is that they consider being universal approximators of functions (e.g., [17]-[21]).

Thus, artificial neural networks (ANN) have been widely used even in the modeling of nonlinear dynamic systems in recent decades, as they have a high capacity to approximate

nonlinear mappings. Several studies have been developed in this area using the NARMAX methodology (Non-linear Auto-Regressive Moving Average with exogenous input) and subsequent application in control (e.g., [22]-[29]).

The historical work that limited the application of artificial neural networks in the late sixties of the twentieth century is due to Minsky (1969) in [30]. Another important old work, but on machine learning, is due to Nilsson (1965) in [31]. Primarily, [5] creates the original work on training a neural network with MLP architecture using the backpropagation algorithm. Besides, [32] complements the first mathematical concepts about the backpropagation. Succeeding, [33] proposes an article on the historical description of this algorithm.

The training algorithm of a neural network with MLP (Multi-Layer Perceptron) architecture known as Marquardt's algorithm and which we use a lot, in all the simulations presented at the end of this article, is due to Hagan (1994) in [6]. Many other algorithms attempt to speed up MLP networks' training, for example, the algorithm described in [34]. After that, the researchers experienced that the theory of neural networks has evolved a lot in the last three decades in an extraordinary way.

The attentive reader must have already realized that the bibliographic references listed at the end of this article are already relatively old (almost all of them are from the nineties of the twentieth century). The reason for this is that this article is a summary of the Master Thesis of Professor Paulo Marcelo Tasinoffo, carried out in 1998 in Brazil (see [35]). Its advisor was Professor Afonso Henriques Moreira Santos (first author of this article).

Therefore, this article went unpublished for more than 20 years. In this way, we prefer, as far as possible, to leave the original references for the preparation of this thesis. We just added recent contributions from articles that combine the Monte Carlo method with artificial neural networks. Another important observation is that the software developed still needs to undergo a restoration process since it was established in the late nineties using Windows 95. For example, the Moody diagram interpolated by neural networks (see section IX and Figure 7) could be significantly improved nowadays.

To conclude this section, it should note that both Monte Carlo Methods and the theory of artificial neural networks are very vast fields of science and mathematics. The ability to combine these two branches of mathematics (e.g., [13]-[14]) can be seen in some recent modern articles. This capacity makes the technological application of artificial neural networks increasingly broad in solving current engineering problems.

III. THE MONTE CARLO METHOD

A forced hydraulic system of drinking water supply with n consumers develops a random and non-deterministic manner water consumption. Statistical systems simulation methods can adjust adequately to the problem described and, therefore, choosing to be applied in this work.

The Monte Carlo method is characterized by a high number of computer simulations to obtain statistical results. For this to be possible, remain a set of temporal samples of the elements involved in the simulation must initially. Thus, for a set of n

elements with m temporal samples in each element, the initial Table 1 of data can be formed. The elements in Table 1 form a data matrix of n consumers of a drinking water supply network, with the respective drinking water consumption being accounted for or measured monthly for m consecutive months.

However, there is a possibility to measure the consumption of drinking water by consumers, using a period shorter than one month. For example, measurements could be performed two or even four times a day to obtain a more reliable statistical result, at least for the first hydraulic installation studied. The other hydraulic fittings, which come after the first installation studied exhaustively, could use the transposition of the results of the first one to make the measurements easier. These results will be made more evident in section IV. Thus, with the samples in Table 1, the vector of the means (μ_Q) of the n elements and the variance-covariance matrix (Σ_Q) of the samples must be obtained. These expressions are given respectively by:

$$\mu_Q = \begin{bmatrix} \frac{Q_{11} + Q_{21} + \dots + Q_{m1}}{m} \\ \frac{Q_{12} + Q_{22} + \dots + Q_{m2}}{m} \\ \vdots \\ \frac{Q_{1n} + Q_{2n} + \dots + Q_{mn}}{m} \end{bmatrix} = \begin{bmatrix} Q_1 \\ Q_2 \\ \vdots \\ Q_n \end{bmatrix}, \quad (1.a)$$

$$\Sigma_Q = \begin{bmatrix} \sigma_{11} & \sigma_{12} & \dots & \sigma_{1n} \\ \sigma_{21} & \sigma_{22} & \dots & \sigma_{2n} \\ \vdots & \vdots & \ddots & \vdots \\ \sigma_{n1} & \sigma_{n2} & \dots & \sigma_{nn} \end{bmatrix}, \quad (1.b)$$

to

$$\sigma_{ij} = \frac{1}{m-1} \cdot \sum_{k=1}^m (Q_{ki} - Q_i) \cdot (Q_{kj} - Q_j), \quad (1.c)$$

where, $i = 1, 2, \dots, n$ e $j = 1, 2, \dots, n$.

For the particular case of this work, Q_{mn} represents the n th consumer's water flux at the m th instant. The water fluxes of consumers can be determined indirectly from the water meters installed in all homes in the neighborhood studied.

Table 1. Set of temporal samples of the elements to be involved in the simulation.

	Element 1	Element 2	...	Element n
Instant 1	Q_{11}	Q_{12}	...	Q_{1n}
Instant 2
.
.
Instant m	Q_{m1}	Q_{m2}	...	Q_{mn}

Thus, in possession of (μ_Q) and (Σ_Q), the behavior for each element, as well as the entire hydraulic system, can be predicted by the Monte Carlo method. For the variances and covariance to be respected, a procedure as described below is necessary.

Let W be the vector of the random variables representing

the behavior of the n elements of the set at a given instant, however, for the particular case in which $\Sigma_Q = \Sigma_w$ and $\mu_w = 0$ (null vector), that is, variables centered on zero. It is possible to write the expression (2), where Z is a vector of n normal, standardized and independent random variables, and Y a matrix whose elements (y_{ij}) must be calculated for the identity (2) to be valid.

$$W = Y \cdot Z, \quad (2)$$

Hence, it can be proved that the variance-covariance matrix of W (Σ_w) is given by property (3), where Σ_Z is the variance-covariance matrix of Z .

$$\Sigma_w = Y \cdot \Sigma_Z \cdot Y', \quad (3)$$

The variable Y' denotes the transposed matrix of Y . Matrix Σ_Z is the identity matrix of order $n \times n$ since it belongs to a sample of independent standardized n normals. Like this,

$$\Sigma_w = Y \cdot Y' = \Sigma_x, \quad (4)$$

It is now possible, through expression (4), to calculate the elements of Y . However, there are infinite solutions. To facilitate the calculation, Y is assumed to be triangular, and thus, Y is determined by the Forward Substitution method. With the Y matrix, we return to expression (2). Values are drawn for the n variables y (independent normals), and the n variables z are calculated. Adding the respective mean values of the vector μ_Q we have a set of simulated data for individual consumption:

$$Q = W + \mu_Q, \quad (5)$$

By carrying out a large number of drawings, that is, obtaining several Q vectors, it is possible to study the system's typical behavior in its aspects of interest. The Monte Carlo method can then be defined as the successful realization of several drawings to obtain several Q vectors that must obey equality (5).

IV. TRANSPOSITION OF RESULTS

A first data collection was carried out for a specific hydraulic system for drinking water supply. From these results and the use of statistics, it is possible to predict a probability density function (pdf) that best characterizes the system. This technique (pdf) generalize the behavior of hydraulic systems, to a certain extent, similar to the first. In this way, the prediction of consumers' behavior from other installations can be obtained without the need for new data collections.

However, it should be kept in mind that the more extensive and more diverse the samples are, the more accurate the (pdf) obtained will be. Therefore more reliable results can be acquired for the other hydraulic installations. Considering now the methodology of transposing the results, correctly said. The previous knowledge of the mean vector (μ_Q) and the variance-covariance matrix (Σ_{μ_Q}) of the initial installation already studied, represented by equations (1.a) and (1.b), are crucial. Then, based on these values, the unit matrix of the system is calculated, as illustrated in equation (6).

It is important to note that this equation (6) is a generalization of the initial hydraulic installation's statistical behavior and studied exhaustively. In this way, it can be used

as a good approximation for other hydraulic installations. The only necessary information to be known should be the monthly consumption of drinking water. A preliminary study indicates that these statistical distributions are not very different from traditional Gaussian distributions.

The mean water fluxes that appear in equation (6) refer to the monthly consumption of drinking water. Thus, consumers of the initial hydraulic installation must be thoroughly studied to obtain an adequate and accurate data matrix in (6).

$$\dot{\Sigma}_{\mu Q} = \begin{bmatrix} \frac{\sigma_{11}}{\bar{Q}_1 \cdot \bar{Q}_1} & \dots & \frac{\sigma_{1n}}{\bar{Q}_1 \cdot \bar{Q}_n} \\ \dots & \dots & \dots \\ \frac{\sigma_{n1}}{\bar{Q}_n \cdot \bar{Q}_1} & \dots & \frac{\sigma_{nn}}{\bar{Q}_n \cdot \bar{Q}_n} \end{bmatrix}, \quad (6)$$

Where, $\dot{\Sigma}_{\mu Q}$ is the unit variance-covariance matrix of the system.

In this way, the elements of the matrix can be divided into two categories of elements: the first being the set of elements on the main diagonal and the second being the set of elements or below or above the main diagonal. Thus, the following auxiliary vectors are obtained.

$$\dot{\sigma}^2 = \left\{ \begin{matrix} \bullet \\ \sigma_{11}, \sigma_{22}, \dots, \sigma_{nn} \end{matrix} \right\}, \text{ to } \sigma_{ii} = \frac{\sigma_{ii}}{\bar{Q}_i \cdot \bar{Q}_i}, \quad (7.a)$$

$$\dot{\sigma}_{ij} = \left\{ \begin{matrix} \bullet \\ \sigma_{21}, \sigma_{31}, \dots, \sigma_{1n}, \dots, \sigma_{nn-1} \end{matrix} \right\}, \text{ to } \sigma_{ij} = \frac{\sigma_{ij}}{\bar{Q}_i \cdot \bar{Q}_j}, \quad (7.b)$$

The vectors (7.a) and (7.b) must have a distribution of probabilities $\hat{\sigma}_{ii}$ and $\hat{\sigma}_{ij}$, respectively. An example of a probability distribution to illustrate the model is presented in Figure 2. To obtain the probability distributions $\hat{\sigma}_{ii}$ and $\hat{\sigma}_{ij}$, the histogram of the vectors (7.a) and (7.b) must first be obtained and determined.

Since the vectors presented in the last two equations represent the system's best probability distributions, they can be used to generate the flux of drinking water typical of the n consumers of any hydraulic installation. However, these vectors are by no means self-sufficient, and some minimal and necessary information about the new system must still be known. For this particular case, knowledge of the vector of mean monthly fluxes of drinking water from consumers (μ_Q^2) and the physical and geometric configuration (isometric) of the new hydraulic installation will also be crucial.

With this information, it is possible to draw a new unit variance-covariance matrix and determine the variance-covariance matrix of the new system and, as indicated in equation (8). In equation (8), the mean drinking water consumption values of the new hydraulic installation where the results are to be transposed are used.

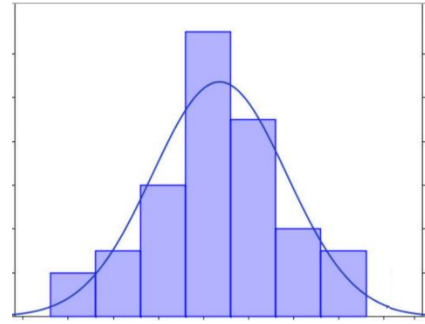


Fig. 2 A graphical example of a particular type of probability distribution and the histogram that generated it.

$$\Sigma_{\mu Q^2} = \begin{bmatrix} \bullet & & \bullet \\ \sigma_{11} \cdot \bar{Q}_1 \cdot \bar{Q}_1 & \dots & \sigma_{1m} \cdot \bar{Q}_1 \cdot \bar{Q}_m \\ \dots & \dots & \dots \\ \bullet & & \bullet \\ \sigma_{m1} \cdot \bar{Q}_m \cdot \bar{Q}_1 & \dots & \sigma_{mm} \cdot \bar{Q}_m \cdot \bar{Q}_m \end{bmatrix}, \quad (8)$$

Where, $\Sigma_{\mu Q^2}$ is the variance-covariance matrix of the new hydraulic installation; \bar{Q}_i is the i-th element of the mean vector (μ_Q^2) of the monthly fluxes of the m consumers of the new hydraulic network and $\dot{\sigma}_{ij}$ are the elements generated randomly from the unit distribution found for the original system.

It should be noted that these last elements, generated randomly, are not the unit values found for the first model, but random values drawn from these. With the vector (μ_Q^2), the variance-covariance matrix ($\Sigma_{\mu Q^2}$), and the physical and geometric configuration of the new hydraulic system, then it will be possible to apply the Monte Carlo method, as explained in section III of this work. Thus, it will be possible to consolidate and simulate the new hydraulic system's behavior, just as it was done for the original hydraulic system.

V. ARTIFICIAL NEURAL NETWORKS AS UNIVERSAL APROXIMATORS OF NONLINEAR FUNCTIONS

Artificial neural networks can be defined as an interconnection of neurons, such that the outputs of a neuron are connected via weights, to all other neurons in the network, including itself (see [4] and [15]). This is the best definition of neural networks in terms of computation. It can be proved that artificial neural networks with feedforward architecture can function, from the mathematical point of view, as universal approximators of functions.

Train a neural network is nothing more than solving an optimization problem [4]. This problem can be seen as a nonlinear least squares problem. The backpropagation rule is used to determine the Jacobian of the network and, thus, it can be applied to conventional methods of numerical optimization, such as, for example, the gradient method.

Since the backpropagation training algorithm (see [5]) was popularized, much research has been done to accelerate the convergence of its application to real problems. The Marquardt algorithm (see [6]) has a faster convergence than conventional backpropagation, when the number of weights

in the network is less than a few hundred. Thus, it was decided to use this last algorithm in the elaboration of the trainings used in this article.

Artificial neural networks were used here for the interpolations of the hill diagram of the centrifugal pump tested in the laboratory (see Figures 3 and 6) and of the Moody diagram (Figure 7) that determines the friction factor of pipes in the calculation of pressure loss.

VI. HILL DIAGRAM OF CENTRIFUGAL PUMPS

To analyze the system where there is variation in the rotation of the motor-pump set, one should first understand the hill diagram that relates the physical quantities Q_b (pump flux), n_b (pump rotation), H_b (total pump height) and η_b (pump performance). Figure 3 illustrates how the general diagram of such equipment is composed.

As can be seen, the lines ($n1, n2, n3, n4$) represent the various rotations admitted by the system. The increase in rotation will always occur from left to right, that is, $n1 < n2 < n3 < n4$ for any pump.

The constant hydraulic performance curves are represented by the closed elliptical curves in the diagram. Hydraulic performance has always increased from outside to inside the diagram, that is, there is always $\eta_1 > \eta_2 > \eta_3 > \eta_4$.

The curves ($\alpha_1, \alpha_2, \alpha_3$) represent the system for a given configuration and state of a hydraulic network. State, in this case, is understood to mean mainly the position of consumers' valves (water tank buoys, etc.). For the case where the system works with these valves fully open, the system curve is represented by the curve α_1 , and when these valves are closed, the curve tends to be more pronounced and will, for example, be represented by α_2 . That is, the curve of the system will depend on the geometry and configuration of the piping of its hydraulic elements (elbows, valves, etc.) and on the current status of each hydraulic element (closed, partially open or fully open).

In this way, if the pump is activated to work with a rotation n_2 , imposed by the electric motor, and α_1 being the typical operating curve of the system, then the operating point of the motor-pump set will be given by the equilibrium point of these two curves, which can be mathematically represented by their intersection in the hill diagram.

Still based on Figure 3, assume that the pump is running at a flux rate Q_{b1} and a total height H_{b1} . Changing the pump rotation from n_1 to n_2 , keeping the flux constant, it is observed that there is an increase in the performance of the motor-pump set, but there is also an increase in the total height required by the pump from H_{b1} to H_{b2} . As the equations below show, with a simultaneous increase in H_b and η_b , it is not possible to say whether there is an increase or decrease in the electrical power required by the hydraulic system.

$$P_m = \rho \cdot g \cdot Q_b \cdot H_b, \quad (9.a)$$

$$P_{el} = \frac{P_m}{\eta_t}, \quad (9.b)$$

where, η_t is the total performance of the motor-pump system and P_m is the mechanical power of the motor-pump system.

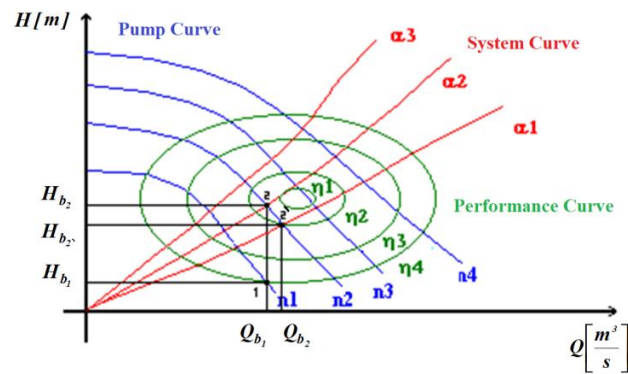


Fig. 3 Schematic representation of the hill diagram of the motor-pump set.

Another detail to be analyzed in this system is the increase in H_b . Due to the increase in system speed, the pump flux is not kept absolutely constant, but it does increase. This can be easily explained, because when there is an increase in the total pressure of the pump it is immediately passed on to the system, slightly increasing its flux rate. In this way, the final balance of the system will be reached only in Q_{b2} and H_{b2} and as shown in Figure 3. As the n_2 rotation has not changed, the new equilibrium point of operation of the pump will finally be in $H_{b2'}$ and no longer in H_{b2} . Thus, the system will reach a new equilibrium point at 2'. Note, that in this case, there was a small decrease in pump performance. This exemplifies that the energy balance of hydraulic pumping systems is not trivial and extremely non-linear. All this information about the hill diagram is very important to understand the algorithm stated in section VIII.

VII. DETERMINING THE SYSTEM'S LOSS OF LOAD

The calculation of the head loss in hydraulic installations for pumping drinking water (e.g. [1] - [3]) is a very important part of the simulation model presented in this work.

At the point of escape, in each of the n consumers, the pressure can be easily calculated. Let Z_i be the level between the i -th consumer and the centrifugal pump, H_{b1} the total height of the pump and $(p_1+p_2+\dots+p_p)$ the pressure drop between the i -th consumer and the pump, in this way we have:

$$H_{ci} = H_{b1} - \sum_{j \in L} p_j - Z_i, \quad (10)$$

where, H_{ci} is the supply pressure on the i -th consumer; H_{b1} is the total height of energy supplied by the pump; $\sum_{j \in L} p_j$ is the

pressure drop in the piping between the pump output and the i -th consumer; L is the set of all tubes that connect the pump to the i -th consumer and Z_i is the existing level between the pump and the i -th consumer.

In this way, applying equation (10) to all n consumers in the network, it is possible to evaluate supply pressures for consumers. This fact will make it possible to evaluate a region or group of consumers who have pressure that is either too high or too low, in addition to energy waste points. The crucial question now is to determine head loss of consumers. Thus, all flow around a pipe is subject to a pressure drop that is a function of the Reynolds number:

$$Re = \frac{\rho \cdot v \cdot D}{\mu} = \frac{v \cdot D}{\nu} \quad (11)$$

where, Re is the Reynolds number [dimensionless], ρ is the specific mass of the fluid measured in the unit $[\text{kg}/\text{m}^3]$; ν is the velocity of the fluid in $[\text{m}/\text{s}]$; μ is the absolute viscosity in $[\text{kg}/\text{m}\cdot\text{s}]$; ν is the absolute viscosity in $[\text{m}^2/\text{s}]$ e D is the diameter of the tube in $[\text{m}]$. For circular cross-section tubes, the Reynolds number can be expressed by:

$$Re = \frac{4}{\pi} \cdot \frac{Q}{d \cdot \nu} \quad (12)$$

The mean values of absolute roughness are called equivalent or effective rugosities (ε). Thus, the following expression valid for any liquid or fluid can be verified experimentally:

$$\Delta h = f \cdot \frac{L}{D} \cdot \frac{v^2}{2 \cdot g} \quad (13)$$

where, Δh is the head loss measured in $[\text{m}]$ between points a and b of a given pipe; ν is the flow velocity in $[\text{m}/\text{s}]$; f is the fluid friction coefficient [dimensionless]; L is the total length of the pipe in $[\text{m}]$; D is the pipe diameter in $[\text{m}]$ and g is the acceleration of local gravity in $[\text{m}/\text{s}^2]$. For computational purposes it is more convenient to express equation (13) as a function of the flux (Q) and not the speed (ν) of the fluid. Thus, we have:

$$\Delta H = 0.0826 \cdot f \cdot L \cdot \frac{Q^2}{D^5} \quad (14)$$

Equation (14) provides the head loss in a circular cross-section pipe of length L , diameter D and flux Q . The only drawback of this equation is the determination of the friction factor (f). This is a dimensionless coefficient that is a function of the Reynolds number (Re) and the relative roughness (ε/d). Thus, to determine the factor f there are several ways: Blasius, Karman-Prandtl, Nikuradse, Colebrook and others equations. However, these methods are generally made up of a set of equations and not a single equation for performing that calculation. So it is difficult for the computer to decide which one to choose in each case.

For this reason, the method used here was to interpolate the Moody Diagram (see Figure 7) through artificial neural networks. The Moody diagram (1944) is a logarithmic scale graph with the Reynolds number (Re) represented in the abscissa and in the ordinates the relative roughness (ε/d). Once these values are known, it is possible to read the friction factor of the pipe. In order for this diagram to be used correctly, it has been divided into three distinct regions:

a) For $Re < 2000$ the regime is considered laminar and the Poiseuille equation can be used in this situation:

$$f = \frac{64}{Re} \quad (15)$$

Note that, in this case, the friction coefficient does not depend on the relative roughness.

b) For Re between 2000 and 4000 the flow will have an unstable or critical transition regime from laminar to turbulent. In this case, in particular, the friction factor oscillates around a curve that can be considered independent of the relative roughness.

c) For $Re > 4000$, the regime will be turbulent and then, the friction coefficient (f) will depend on the number of Reynolds

and the relative roughness. This case is extremely non-linear and ideal for being represented by a neural network. However, when the turbulence is complete (Reynolds very high) then f will depend only on the relative roughness.

The only drawback to be solved now is with respect to localized losses (e.g., pipe elbows, etc.). To solve this last problem, the concept of equivalent length over a physical element present in a pipe will be used. For example, an elbow that has a head loss J will have an equivalent length L , such that, if it were a pipe, it would have the same head loss J . Thus, this concept can be generalized to the other physical elements present in a pipe.

In this way, knowing the equivalent length of a localized element of the pipe, then it can be treated as a pipe and, therefore, equation (14) can be applied on it as well. Therefore, the calculation of the head loss can be determined by the entire length of the pipe.

VIII. FULL ALGORITHM

In this section, we present the complete computational algorithm used to simulate the energy balance of the motor-pump system operating at variable speed. The steps of this algorithm are as follows:

1) The flux (Q_{11} , Q_{21} , ..., Q_{n1}) of the n consumers of the network are drawn using the Monte Carlo Method, as explained in section III, storing them in a vector. The second index of the elements of the flux vector indicates the initial values of the same and which must be corrected if the system changes its rotation. The sum of all these fluxes will provide the initial pump flux, that is:

$$Q_{b1} = \sum_{i=1}^n Q_{i1} \quad (16)$$

2) The output pressure of the n consumers is calculated using the equation below:

$$H_{ci1} = H_{b1} - \sum_{j \in I} p_j - Z_i \quad (17)$$

This way, for the initial flux vector of the n consumers of the system (Q_{11} , Q_{21} , ..., Q_{n1}) and for an initial rotation (n_1) of the pump, we have the corresponding initial supply pressure vector, also with n elements, represented by (H_{c11} , H_{c21} , ..., H_{cn1}). It is important to note that knowledge of the pump diagram (see section VI) is of fundamental importance, in this part of the algorithm, to obtain H_{b1} from n_1 and Q_{b1} . The head loss calculation can be determined as explained in section VII.

3) To incorporate the effect of changing the pump rotation, for example, from n_1 to n_2 , the following correction of the supply pressures is made for each of the n consumers:

$$H_{ci2} = H_{ci1} + (H_{b2} - H_{b1}) \quad (18)$$

This will provide a second pressure vector (H_{c12} , H_{c22} , ..., H_{cn2}) for this hydraulic system. Note that H_{b2} can be obtained from the hill diagram, interpolated by the artificial neural network, simply from n_2 and Q_{b1} .

4) The second flux vector for the n consumers of the network is generated. This is done based on the vectors obtained in steps 1, 2 and 3 and replaced by the mathematical relation expressed below:

$$\left(\frac{Q_{i2}}{Q_{i1}}\right)^2 = \frac{H_{ci2}}{H_{ci1}}, \quad (19)$$

This expression evaluates the behavior of the consumer system, whose valve associated with the float is the main element. Thus, exponent 2 is a good approximation, but it is not a definitive value, requiring further studies.

The sum of all the elements of the new vector representing the flux of consumers ($Q_{12} + Q_{22} + \dots + Q_{n2}$) will be equal to the new flux Q_{b2} of the pump. This is in accordance with common sense, since the flux of the pump must change with the variation of the pump.

5) The vector ($H_{c12}, H_{c22}, \dots, H_{cn2}$) represents the output pressures of the n consumers still with pump flux in Q_{b1} . Thus, a new output pressure vector ($H_{c12}, H_{c22}, \dots, H_{cn2}$) must be found that considers the new flux Q_{b2} . This can be done relatively easily.

Based on the new flow Q_{b2} and the new rotation n_2 , H_{b2} is determined through the hill diagram, again using the interpolation by artificial neural networks. In this way, there will be two distinct situations:

If $(H_{b2} - H_{b1}) > \text{admitted error}$, then we return to step 3 of the algorithm and with the new pressure, the consumer pressures are recalculated and, therefore, the flux of each one. The new pump flux is then calculated and, with the same speed n_2 , the new H_b is obtained. This must be done until this condition is satisfied, in which case the condition below will finally be increased.

If $(H_{b2} - H_{b1}) < \text{admitted error}$, then in possession of H_{b2} and the flux vector ($Q_{12}, Q_{22}, \dots, Q_{n2}$) the new consumer output pressures are recalculated by the following expression:

$$H_{ci2} = H_{b2} - \sum_{j \in J} p_j - Z_i, \quad (20)$$

At this point in the algorithm, the consumer flux vectors ($Q_{12}, Q_{22}, \dots, Q_{n2}$) and the consumer supply pressure ($H_{c12}, H_{c22}, \dots, H_{cn2}$) are already known for the new system rotation. The values of Q_{b2} and H_{b2} are also known and, thus, the energy analysis of the system can be started. However, before that, a summary of the tasks performed by this algorithm will be presented.

a) The initial behavior of consumers is evaluated using the Monte Carlo method, generating flux vectors for consumers Q_{i1} and supply pressure for consumers H_{ci1} . In this situation, it can be said that the system is operating with the pump at one rotation (n_1), at a flux rate (Q_{b1}) and at a total height of energy (H_{b1}).

b) The rotation of the system is varied from n_1 to n_2 . Thus, for the same consumers generated in step (a), it generates the new behavior of the system expressed by the new flux vectors of consumers Q_{i2} and supply pressure of consumers H_{ci2} . In this new state of operation the system has its pump operating at one rotation (n_2), at a flux rate (Q_{b2}) and at a total height of energy (H_{b2}).

Based on steps (a) and (b) it is observed that there is all the necessary data to perform an energy analysis of the system, both before and after the variation of the pump rotation. This will allow to evaluate and to compare the two states of the system. After carrying out the previous simulation, the mechanical powers before and after the variation of the pump speed can be calculated respectively as follows:

$$P_{e1} = \rho \cdot g \cdot Q_{b1} \cdot H_{b1} / \eta_{t1}, \quad (21.a)$$

$$P_{e2} = \rho \cdot g \cdot Q_{b2} \cdot H_{b2} / \eta_{t2}, \quad (21.b)$$

Note that the hydraulic performances (η_t) are taken from the hill diagram and corresponding to the respective operating point. As already mentioned, the Monte Carlo method requires that the system be simulated a high number of times. In this way, this will allow to evaluate the optimum power of the system.

That said, a new simulation is carried out using the previously presented algorithm, repeating its 5 steps previously described. Thus, the new powers for this second simulation are obtained from equations (21.a) and (21.b). If this procedure is repeated k times, there will be k hydraulic powers before the variation of the pump rotation and k hydraulic powers after the variation of this rotation. Thus, the mean power of the system before and after the variation of the pump speed will be respectively given by:

$$\bar{P}_{h1} = \frac{1}{k} \cdot \sum_{i=1}^k P_{h1k}, \quad (22.a)$$

$$\bar{P}_{h2} = \frac{1}{k} \cdot \sum_{i=1}^k P_{h2k}, \quad (22.b)$$

However, the volume of total water consumed is the same both for the initial situation of the system and for the case where the pump rotation variation occurred. Thus, the mean power given by equation (22.b) must have a correction term, since the pump's operating time is different for both cases. Thus, as the volume consumed is constant we have:

$$t_2 \cdot Q_{b2} = t_1 \cdot Q_{b1} = \text{total volume consumed} \quad (23.a)$$

or

$$\frac{t_2}{t_1} = \frac{Q_{b1}}{Q_{b2}}, \quad (23.b)$$

On the other hand, the total energy of the system is represented, respectively, before and after the variation of the pump rotation, by:

$$E_1 = P_{h1} \cdot t_1, \quad (24.a)$$

$$E_2 = P_{h2} \cdot t_2, \quad (24.b)$$

Representing the total energies of the system by E_1 (before the variation of rotation) and E_2 (after variation of rotation), for the same time interval, we have:

$$E_2 = \bar{P}_{h2} \cdot \frac{Q_{b1}}{Q_{b2}} \cdot t_1, \quad (25)$$

Now, as the last step to correct the hydraulic power to be determined for the system working with variable rotation, we must still perform one last mathematical artifice.

Thus, observing Equation (25) it can be concluded that the mean power \bar{P}_{h2} must be multiplied by the factor $\frac{Q_{b1}}{Q_{b2}}$ to be valid at the same interval t_1 of the initial situation. So, we finally have to:

$$\bar{P}_{h2} = \frac{1}{k} \cdot \sum_{i=1}^k P_{h2k} \cdot \frac{Q_{b1k}}{Q_{b2k}}, \quad (26)$$

It should be noted that, to perform the comparison between the mean powers before and after the variation of the pump

rotation, they must be represented in the same time interval, in this case, t_j .

IX. RESULTS ACHIEVED IN NUMERICAL SIMULATIONS

In this section, the graphical results obtained in the simulation of the pumping system with variable rotation are presented for a typical and real case in the supply of drinking water in the Vista Verde neighborhood existing in the city of Itajubá/Brazil. The chosen installation is a pumping station type in march. The city's main reservoir, which is at an altitude of 899 [m], feeds the pump suction reservoir at 850 [m] by gravity. Figure 4 shows a sketch of the Vista Verde lift station.

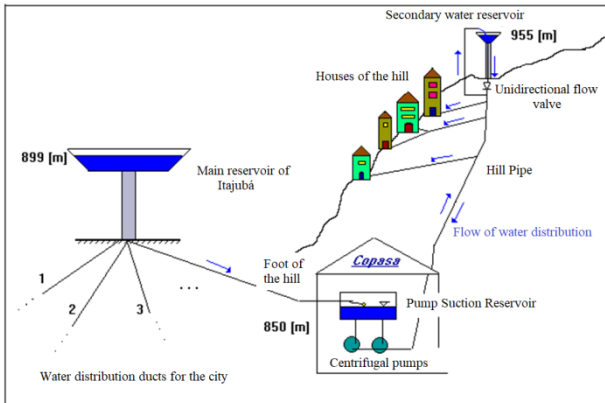


Fig. 4 Pumping station in the Vista Verde neighborhood.

The pump's suction reservoir has a float valve to control its level. The pumps are installed below the level of the reservoir, which characterizes being drowned, very common in this type of installation in Brazil. In the suction line of each pump, with a diameter of 4", a gate valve is installed that remains open in the assembly that is in operation and closed in the reserve. In the case of the repression line with a diameter of 3", each pump at its output has a gate valve, which always remains open.

A little above the pump output, a Bourdon-type pressure gauge and a pressure switch are installed that turn the assembly off when the pressure reaches 12 kg / cm². The pump feeds the main line of the neighborhood, towards its reservoir at elevation 955 [m]. In this sense, there is distribution to consumers. The line has a "by pass" that feeds the reservoir and a unidirectional valve that, in return, serves consumers by gravity.

The pump turns on again through a timer control, installed on the electrical panel, two hours after shutdown. There are 78 houses mirrored on the hill where the Vista Verde neighborhood is located. The reading of the hydrometers, of the residences that are supplied by the pumping system, is also necessary for the simulation. As the number of houses in this neighborhood is relatively small, this facilitated data collection.

Figure 5 shows the schematic of one of the four stage pumps inside the lift station machine room. The drowned pump sucks water from the reservoir and presses it back to the main distribution line, where a gate valve is installed at the pump output, which always remains open, and a Bourdon pressure gauge for reading the output pressure. The motor that drives the pump is a monoblock type.

Figures 6 and 7 represent, respectively, the results obtained by the neural training of the hill diagram of the centrifugal pump in the Vista Verde neighborhood and the Moody diagram for the determination of pressure losses. As seen in the previous sections, these two diagrams are very important for the execution of the algorithm presented in section VIII. Figure 8 is an aerial view of the UNIFEI University Campus where the hydraulic tests were carried out to obtain experimentally the hill diagram shown in Figure 6, which was later interpolated by artificial neural networks.

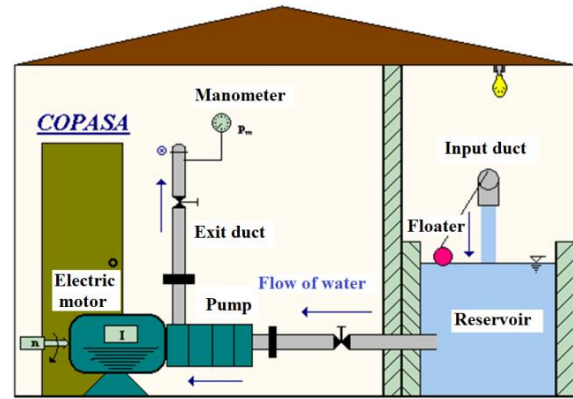


Fig. 5 Machine room of the Vista Verde pumping station.

Figure 9 shows the graphic entry of the hydraulic drinking water supply in the graphic editor, which is one of the integral parts of the developed simulator. The graphical interface of the software in Figure 9 was originally developed in Portuguese. Also note that the black background is still an inheritance of the old DOS environment, still with little use at the time of Windows 95. Figure 10 shows the results of a Monte Carlo simulation with the hydraulic system working at variable speed. These results follow the criteria as presented by the algorithm in section VIII. Figure 11 shows a simulation for the same hydraulic installation. The difference here is that the system is working with constant rotation.

Comparing the two graphs present in Figures 10 and 11, it can be seen that the variable rotation system works with a mean mechanical power equivalent to only 80.23% of that required for the system working with constant rotation. This is an important indication that a control of drinking water pumping at variable rotation in a hydraulic installation with several consumers present is a good option regarding the aspect of energy conservation and financial savings in the electricity bill for the company COPASA, provider of this type of service. However, for this an initial economic investment for the purchase of frequency inverters, digital computers and additional sensors will be necessary.

This application has some restrictions that will be mentioned below. It is important to consider this information when simulating the system, so that the software in question is not misused. These limitations are:

- 1) All hydraulic installation tubes are admitted to have a circular cross section;
- 2) Located elements of the valve type (drawer, globe, check, etc.) were not considered in the elaboration of this simulator;
- 3) The coupling elements of the tee and cross type are all considered to have an inclination of 90 degrees (if these elements, of the installation to be simulated, do not have this

inclination angle, then they should be approached to 90 degrees);

4) Elbows can have slopes of 90 or 45 degrees (slopes outside these values cannot be used);

5) It is only possible to simulate a hydraulic installation that has a single centrifugal pump (two or more pumps are not allowed by the simulator);

6) If it is desired to use a new centrifugal pump different from the one that this software supports then, a new neural network must be trained with experiments and tests done in the laboratory for the new centrifugal pump considered;

7) The simulator only accepts hydraulic installations with configurations of the fishbone type (ring installations are not allowed).

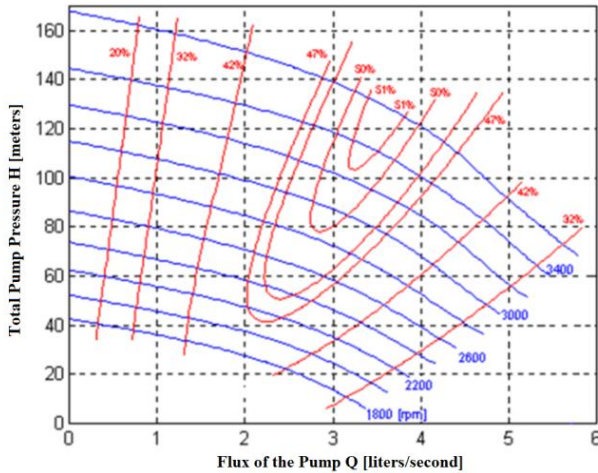


Fig. 6 Hill diagram that represents the basic operating field of the centrifugal pump used in the Vista Verde neighborhood of Itajubá.

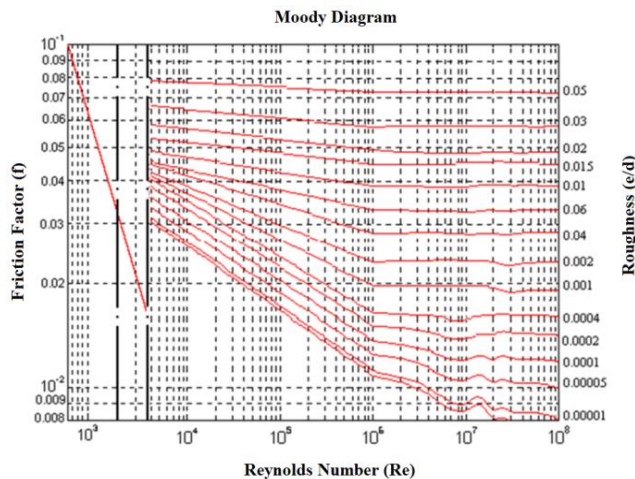


Fig. 7 Interpolation of the Moody diagram by neural network.



Fig. 8 Aerial image of the José Rodrigues Seabra Campus (UNIFEI) in December 2015.

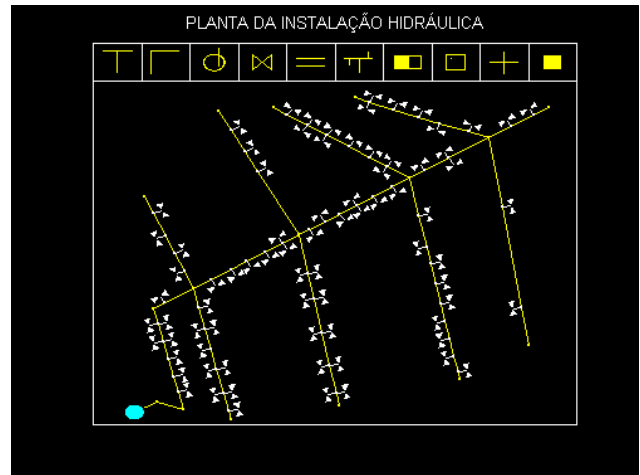


Fig. 9 Isometric of the hydraulic installation in the Vista Verde neighborhood.

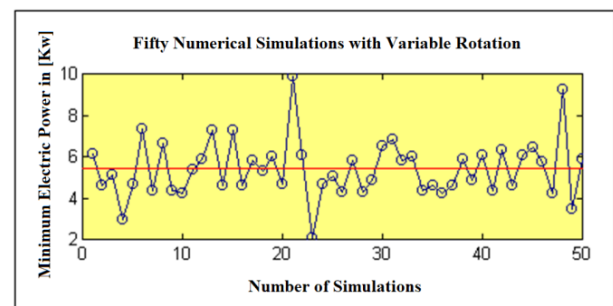


Fig. 10 Monte Carlo simulation with the hydraulic system working with variable rotation.

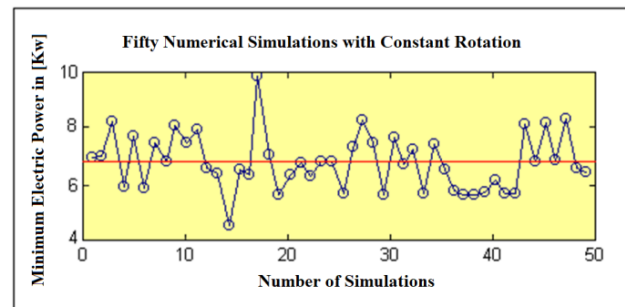


Fig. 11 Monte Carlo simulation with the hydraulic system working with constant rotation.

X. CONCLUSION

The software developed in the Matlab environment was developed with the aim of creating a generic simulator applicable to a very large and distinct range of hydraulic pumping installations, given, of course, the reservations indicate in section IX.

In this way, this simulator can be used not only for the hydraulic installation of the Vista Verde neighborhood located in the city of Itajubá/MG (Brazil), but also for other hydraulic installations, thanks to the mathematical tools used in its elaboration. Therefore, the partial generalization of this simulator was obtained basically thanks to three basic aspects:

1) Use of neural networks for the interpolation of the hill diagram, which describes the basic field of operation of centrifugal pumps;

2) Development of a graphic editor that allows you to recognize the physical and geometric characteristics of a hydraulic installation, simply from the drawing, and from

there, calculate the head loss of the entire hydraulic installation built in the editor (you can also be improved in the future);

3) Application of the transposition of the results to predict the behavior of consumers of hydraulic drinking water networks for those installations other than the hydraulic installation studied and extensively tested in the city of Itajubá/MG (Brazil);

4) The methodology developed here may, in the future, be extrapolated to other types of hydraulic installations, obviously with the improvement and appropriate restoration of the developed software.

ACKNOWLEDGMENT

We thank our colleagues at LHPCH for their support and friendship. To professor Augusto Nelson Carvalho Viana for experimentally obtaining the hill diagram of the centrifugal pump used in the Vista Verde neighborhood, as well as to the students Eduardo Zanirato (for the hydrometric readings taken in the Vista Verde neighborhood in the city of Itajubá/MG located in Brazil). I would like to thank CNPq for the financial support.

We thank PROCEL for the financing of the equipment used and tested during this work. COPASA engineers who allowed experimental tests to be carried out in their hydraulic installations in the city of Itajubá/MG.

We also thank the two engineers from ITA Gabriel Adriano de Melo and Gildárcio Sousa Gonçalves for helping us edit and format this article. In particular, with reverence and admiration we thank for the saving faith of God and for his countless miracles in our daily lives.

REFERENCES

- [1] A. Macintyre, *Bombas e instalações de bombeamento*, Editora Guanabara Koogan, Segunda Edição, Rio de Janeiro, 1987.
- [2] P. Telles, *Tubulações industriais*, Livros Técnicos e Científicos Editora, Quinta Edição, São Paulo, 1979.
- [3] P. Telles, *Tabelas e gráficos para projetos de tubulações*, Editora Inteligência, Terceira Edição, Rio de Janeiro, 1985.
- [4] J. Zurada, *Introduction to artificial neural system*, West Pub. Co., 1992.
- [5] D. Rumelhart, G. Hinton, R. Williams, "Learning representations by back-propagating errors", *Nature*, vol. 323, 1986, pp. 533-536.
- [6] M. Hagan, M. Menhaj, "Training feedforward networks with the marquardt algorithm", *IEEE Transaction on Neural Networks*, vol. 5, no. 6, 1994, pp. 989-993.
- [7] D. Linkens, "Learning systems in intelligent control: an appraisal of fuzzy, neural and genetic algorithm control applications", *IEEE Control System*, vol. 143, no. 4, 1996, pp. 376-386.
- [8] N. Metropolis, S. Ulam, "The Monte Carlo method. Journal of the American Statistical Association", *Taylor & Francis Broup*, vol. 44, no. 247, 1949, pp. 335-341.
- [9] J. Hammersley, *Monte Carlo methods*, Methiren, London, 1964.
- [10] Y. Shreider, *The Monte Carlo method*, Pergamon Press, Oxford, 1967.
- [11] P. Glasserman, *Monte Carlo methods in financial engineering: stochastic modeling and applied probability*, 53. 1 ed., New York: Springer, 2004.
- [12] Papoulis, A. *Probability, random variables, and stochastic processes*, New York: McGraw-Hill, 1965.
- [13] P. Tasinaffo, G. Goncalves, A. Cunha, L. Dias, "Using Monte Carlo method to estimate the behavior of neural training between balanced and unbalanced data in classification of patterns", *Artificial Intelligence Research*, vol. 7, no. 2, 2018, pp. 1-25.
- [14] P. Tasinaffo, A. Santo, E. Junior, C. Forster, R. Shigemura, R. Jacomel, V. Pugliese, B. Iha, A. da Cunha, G. Goncalves, L. Dias, "Determination of forest reserves area using images processed by drones, neural networks and Monte Carlo method", *Mathematics and Computer Science*, vol. 4, no. 6, 2019, pp. 112-129.
- [15] S. Haykin, *Neural networks: a comprehensive foundation*, 2nd ed.,

- New Jersey: Prentice-Hall, Inc., 1999.
- [16] S. Russell, P. Norvig, *Artificial intelligence*, 2nd ed., New Jersey: Prentice-Hall, Inc., 2003.
- [17] G. Cybenko, "Continuous valued networks with two hidden layers are sufficient", Technical Report, Department of Computer Science, Tufts University, 1988.
- [18] K. Hornik, M. Stinchcombe, H. White, "Multilayer feedforward networks are universal approximators", *Neural Networks*, vol. 2, no. 5, 1989, pp. 359-366.
- [19] N. Cotter, "The Stone-Weierstrass and its application to neural networks", *IEEE Transactions on Neural Networks*, vol. 1, no. 4, 1990, pp. 290-295.
- [20] J.-S. Jang, C.-T. Sun, E. Mizutani, *Neuro-fuzzy and soft computing: a computational approach to learning and machine intelligence*, Prentice-Hall, Inc., 1997.
- [21] J. Spooner, M. Maggiore, R. Ordóñez, K. Passino, *Stable adaptive control and estimation for nonlinear systems neural and fuzzy approximator techniques*, New York: Wiley-Interscience, 2002.
- [22] K. Narendra, K. Parthasarathy, "Identification and control of dynamical systems using neural networks", *IEEE Transactions on Neural Networks*, vol. 1, no. 1, 1990, pp. 4-27.
- [23] S. Chen, S. Billings, "Neural networks for nonlinear dynamic system modelling and identification", *Int. J. Control*, vol. 56, no. 2, 1992, pp. 319-346.
- [24] K. Hunt, D. Sbarbaro, "Neural networks for nonlinear internal model control", *IEE Proceedings - D*, vol. 138, no. 5, 1991, pp. 431-438.
- [25] K. Hunt, D. Sbarbaro, R. Zbikowski, P. Gawthrop, "Neural networks for control systems - a survey", *Automatica*, vol. 28, no. 6, 1992, pp. 1083-1112.
- [26] K. Narendra, "Neural networks for control: theory and practice", *Proceedings of the IEEE*, vol. 84, no. 10, 1996, pp. 1385-1406.
- [27] J. Jarmulak, P. Spronck, E. Kerckhoffs, "Neural networks in process control: model-based and reinforcement trained controllers", *Computers and Electronics in Agriculture*, vol. 18, 1997, pp. 149-166.
- [28] Y. Wang, C. Lin, "Runge-Kutta neural network for identification of dynamical systems in high accuracy", *IEEE Transactions On Neural Networks*, vol. 9, no. 2, 1998, pp. 294-307.
- [29] A. Rios Neto, "Dynamic systems numerical integrators in neural control schemes", V Congresso Brasileiro de Redes Neurais, Rio de Janeiro - RJ, Brazil, 2001, pp. 85-88.
- [30] M. Minsky, S. Papert, *Perceptron*, Cambridge, MA: The MIT Press, 1969.
- [31] N. Nilsson, *Learning machines*, New York: McGraw-Hill, 1965.
- [32] P. Werbos, *Beyond regression: new tools for prediction and analysis in the behavior sciences*, Ph.D. Thesis, Harvard University, Committee on Applied Mathematics, 1974.
- [33] P. Werbos, "Backpropagation through time: what it does and how to do it?", *in Proc. IEEE*, vol. 78, no. 10, 1990, pp. 1550-1556.
- [34] S. Shah, F. Palmieri, M. Datum, "Optimal filtering algorithms for fast learning in feedforward neural networks", *Neural Networks*, vol. 5, no.5, 1992, pp. 779-787.
- [35] P. Tasinaffo, *Regulação de geradores de fluxo pela variação da rotação*, Master Thesis, Universidade Federal de Engenharia de Itajubá (UNIFED), Itajubá/MG, Brazil, 1998.

Afonso Henriques Moreira Santos holds a degree in Electrical Engineering (1978) and a Master's Degree in Mechanical Engineering (1981) from the Federal University of Engineering of Itajubá (UNIFEL) in Brazil. He holds a PhD in Energy Systems Planning (1987) from the State University of Campinas (UNICAMP) also in Brazil and a Post-Doctorate (1991) at the Center International de la Recherche sur l'Environnement et le Développement (CIRED) located in the city of Paris (France). He has over 30 years of experience in the Energy field. He was director of the Brazilian Electricity Regulatory Agency (ANEL) of the Brazilian government from 1997 to 2000.

Paulo Marcelo Tasinaffo has a degree in Mechanical Engineering from the Federal University of Itajubá (UNIFEL, 1996), a Master's Degree in Mechanical Engineering from the Federal University of Itajubá (UNIFEL, 1998) and a PhD in Space Engineering and Technology from the National Institute for Space Research (INPE, 2003). He is currently a professor at the Technological Institute of Aeronautics (ITA) in Brazil. He has experience in the area of Aerospace and Computer Engineering, with emphasis on artificial neural networks, acting mainly on the following topics: modeling of nonlinear dynamic systems, computational mathematics, artificial intelligence, neural control systems, evolutionary computing and stochastic processes.